IEEE Access
Multidisciplinary : Rapid Review : Open Access Journal

Received January 4, 2018, accepted January 31, 2018, date of publication February 13, 2018, date of current version March 15, 2018.

Digital Object Identifier 10.1109/ACCESS.2018.2805684

Numerical Analysis and Optimisation of the Flow Forces in a Water Hydraulic Proportional Cartridge Valve for Injection System

MINGXING HAN, YINSHUI LIU, DEFA WU, HUAIJIANG TAN, AND CHAO LI

State Key Laboratory of Digital Manufacturing Equipment and Technology, School of Mechanical Science and Engineering, Huazhong University of Science and Technology, Wuhan 430074, China

Corresponding author: Yinshui Liu (liuwater@hust.edu.cn)

This work was supported in part by the National Natural Science Foundation of China under Grant 51575200 and Grant 51509097 and in part by the National Key Research and Development Program of China under Grant 2016YFC0300600 and Grant 2016YFC0304800.

ABSTRACT In the applications of the large transient power hydraulic systems, the nonlinear disturbance forces have a significant influence on the performance of the injection system, and it is necessary to take some detail analyses to reduce the influence of the nonlinear disturbance forces. According to the analyses of nonlinear disturbance forces, it can be considered that the flow forces are the major disturbance force. The optimization of the poppet geometry is presented to reduce the axial flow forces. A numerical simulation method is applied to obtain the visualization of the internal flow and achieve a better understanding of the flow field in the valve with double-U-grooves. The main influential geometry parameters of the metering edge were defined and the 3-D computational models were established. Then effects of various parameters on the axial flow forces were studied in detail by using the commercial software ANSYS/Fluent. And the simulation results indicate that the distance between the small U-grooves and the big U-grooves has a major influence on the axial flow forces, and the maximal axial flow forces can be significantly reduced by optimizing the geometry parameters of the valve poppet. Finally, the simulation model of the injection system has been established in AMESim and the simulation results prove that optimum parameters of the poppet can obviously improve the injection performance.

INDEX TERMS Injection system, proportional cartridge valve, computational fluid dynamics, water hydraulics, geometry optimization.

I. INTRODUCTION

Water hydraulic systems that use water as a pressure medium could be a good solution for the environmental and safety problems of the most oil hydraulic systems. Water hydraulic systems have been widely used in the fields of steel and extinguishing and protection, ocean exploration, food and medicine processing, and coal mining [1]–[5]. The die casting technology has been one of the fastest and the most effective methods in manufacturing mechatronics equipment and the precise components for medical, commercial and aviation industrial demands [6]–[7]. However, as so far, most of the die casting machine is driven by oil hydraulics, and has the disadvantages of the pollution due to leakage, flammability and explosion. Compared with the die casting machine powered by oil hydraulics, the die casting machine powered completely by water hydraulic systems has the prominent advantage of environmental protection and safety under high temperature.

In the casting process, the castings quality are closely to many factors, such as mould design (e.g., gate location, runner and cooling channel layout) and injection process parameters (e.g., fast shot velocity, injection pressure, phase changeover point, and holding time). Some advanced die-casting die design systems have been designed to improve the design efficiency and reusing previous design resources [8], [9]. Kumar *et al.* [10] presented a study focused on the optimization for reducing the cold shut defect in casting by using response surface methodology, and the optimized values are validated in confirmation experiments. Deng *et al.* [11] presented a PSO (particle swarm optimization) algorithm for the optimization of multi-class design variables (such as the part thickness, process parameters).

However, the previous studies are primarily focused on tuning the process parameters and mould design (e.g., gate location, runner and cooling channel layout), with less attention on the performance of the injection system of the die casting machine. The high-performance injection system is the foundation of obtaining high-quality castings.

The servo valves and proportional valves are the most important components in the injection system, which have great influents on the dynamical performance of the injection system. The employment of water in hydraulic systems implies a completely different environment for all the mechanical and hydraulic components, different dynamic and lubricating conditions, and this requires a completely or partially modified selection of materials and the design of the hydraulic components [12], [13]. Therefore, a few water hydraulic control valves such as servo valves and proportional valves have already been developed. The shortage of high performance large flow water hydraulic proportional valves is an important factor restricting the application of water hydraulic technology [14]. The dynamic characteristics and control precision of the large flow proportional valve are directly affected by the nonlinear factors such as flow forces, friction forces, inertia forces. In the case of the large transient power hydraulic system, such as injection system of the die casting machine, it is necessary to restrain these nonlinear disturbance factors.

Therefore, to obtain a high response and energy efficient large flow proportional valve, which is suitable for the applications in the injection hydraulic system, the key point is to take some detail analyses to reduce the influence of the nonlinear factors. Herakovic *et al.* [15] indicated that the flow forces would increase with the increase in the volume flow and the pressure different. Therefore, compared with other nonlinear factors, such as friction forces and inertia forces, flow forces have the most significant impact on the characteristics of the large flow proportional valve. Many researchers make use of CFD simulations to analyze the characteristics of the fluid flow and flow forces in valves, and the accuracy of CFD simulation applied to hydraulic valves has been confirmed in many cases [16]–[18]. Simic and Herakovic *et al.* [19] proved that the axial flow forces could be reduced significantly by modifying the geometry of the valve spool and housing. If the optimal geometry of the valve is obtained by experimental analyses, test rigs and test procedures must be developed, and prototypes have to be designed and tested. CFD simulation can provide a better understanding of the flow fields in the valve and avoid the construction and testing of many prototypes during the initial phase of design process. Lisowski *et al.* [20] proposed a method for calculating the flow forces using CFD method on a three-dimensional model and reduced the flow forces by introducing additional parallel and compensatory channels inside the body of valve.

Most current research is focused on the study of mold optimal design and casting process parameters optimal design. However, this study will focus on reducing the disturbance forces through optimizing geometry parameters of the large flow proportional cartridge-type valve. Design of the valve and analysis of nonlinear factors are followed by simulation. In order to design and manufacture the high performance water hydraulic proportional valve, it is necessary to study the characteristics of water hydraulic proportional valve, especially the nonlinear disturbance force (such as flow forces, friction forces and inertia forces) occurred in the large flow of fluid power system. The previous works have proved that the results of CFD simulation agree well with the experiment results on many occasions [21], [22]. Therefore, it will be assumed that the CFD is an appropriate and well accepted tool for evaluating the flow rate and flow forces in this analysis. The present study investigates the flow forces and the flow-pressure characteristics inside the proportional valve used in the injection system. The commercial CFD package, ANSYS/Fluent has been used to carry out all the 3D numerical computations. Finally, the dynamic characteristics of the valve can be improved.

II. INJECTION SYSTEM STRUCTURE AND PRINCIPLE

The injection system, as a kind of typical large transient power water hydraulic system, has a direct effect on the performance of the die casting machine [23]. Accurate injection speed control is an indispensable performance of the advanced die casting machine. If the injection speed is not precisely controlled, the melting metal will not flow uniformly in the mold, thereby resulting in poor casting products which may be caused by shortage of the injected metal, incorrect size or large residual stress. During the injecting process, the powerful hydraulic energy needs to be converted to kinetic energy in a transient period. The proportional valve with high response is one of the most important hydraulic components in the die casting machine, which directly determines the injection speed control performance.

A. INJECTION SYSTEM OF DIE CASTING MACHINE

The structure and principle of the injection system is shown in Fig. 1. The meter-out throttle governing circuit has been used to control the injection speed. At the beginning of the injection process, two-way cartridge directional control valve (7) will be open, and injection accumulator (9) will be connected to head port of injection cylinder (10). The proportional cartridge valve (3) mounted on the rod port of the injection cylinder (10) is used to control the injection speed. Fig. 2 shows the typical injection process [24], [25]. In the process Ls0, plunger past the pour hole at a slow velocity. After the plunger passed the pour hole, the motion of the plunger would be controlled at the ‘‘critical slow shot velocity’’ to eliminate waves and turbulence in the metal for preventing porosity in the process Ls1. Then the next phase Ls2 is the fast shot. The melting metal need to get enough energy to overcome the filling resistance in this phase, and the injection speed is very fast. In the last phase Ls3, injection system would make the plunger rapid braking, and

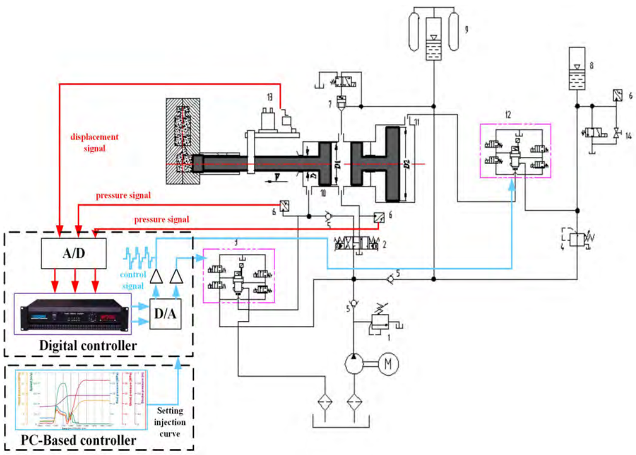

FIGURE 1. Principle of the injection system: 1.relief valve, 2.directional Valve, 3,12.proportional cartridge valve, 4.reducing valve, 5.check valve, 6.pressure transducer, 7.two-way cartridge directional control valve, 8.pressure accumulator, 9.injection accumulator, 10.injection cylinder, 11.booster, 13.displacement transducer, 14. block valve.

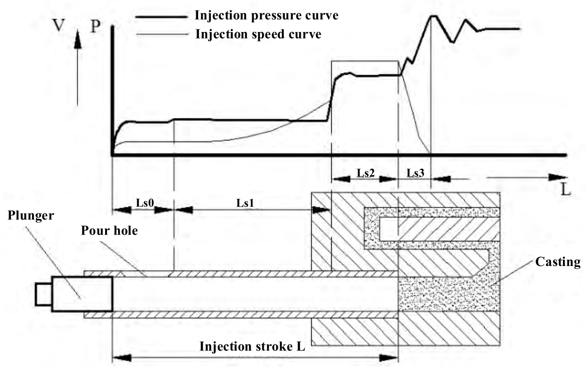

FIGURE 2. Typical injection process.

then increasing the metal pressure to increase casting density and prevent porosity without excessive flash.

The analysis of the injection process shows that the proportional cartridge valve requires high performances, including large flow capacity and accurate flow control and high response, to get the typical injection process. The focus of this research is to investigate the effect of the large flow proportional cartridge valve on the injection process. Therefore, the injection system (as shown in Fig.1) is simplified, and the pressurization control is ignored, as shown in Fig. 3. By a detailed study on the current die casting machine that powered by oil hydraulic, this study chooses medium-sized die-casting machine as an application case for the proportional cartridge valve. The main parameters are shown in table 1.

B. WATER HYDRAULIC PROPORTIONAL CARTRIDGE VALVE

The object of this study is a water hydraulic proportional valve used in die casting machine. In order to meet the demand of large flow and high response for the hydraulic system of the die casting machine, the proportional valve needs to have high flow capacity. In the present research,

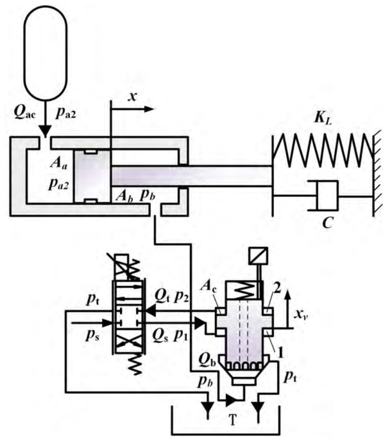

FIGURE 3. The simplified the model of the injection system.

TABLE 1. The main parameters of die casting machine.

parameters	value
Locking force F	5000 N
Hydraulic system pressure Ps	16 MPa
Maximum injection speed Vmax	10 m/s
Slow injection speed Vmin	0.1-0.8m/s
Diameter of plunger rod D	88 mm
Diameter of injection cylinder D1	120 mm

the two-stage or three-stage structure is an attractive solution to achieve a high flow capacity, and there were literatures on multi-stage structure used in proportional/servo valve. Xu *et al.* [26] proposed a three-stage structure directional valve for the large transient power hydraulic system. In order to overcome the fundamental trade-off between the flow capacity and response, two high-speed on/off solenoid valves were used as the pilot stage and two cartridge poppet valves as the secondary stage. The traditional large flow proportional cartridge valve uses a 4/3-way slide-type proportional/servo valve as the pilot valve [27], [28]. Compared with the sliding valve, poppet valve has greater advantages on the sealing performance and manufacturability for the water hydraulic system [29]. Considering the requirement of high frequency and large flow for the die casting machine, a two-stage valve is presented in this study. As shown in Fig.4, four high response 2/2-way water hydraulic proportional valves are used as the pilot stage and a cartridge poppet valve with notches are utilized as the main stage. The four pilot valves have been installed on the connection plate, and connected with the main valve. The pilot stage that consists of four 2/2-way water hydraulic proportional valves has the same control function as the 4/3-way slide-type proportional/servo valve.

Fig. 4 shows the principle of the water hydraulic proportional cartridge valve. The hydraulic bridge consists of four pilot valves, which controls the motion of the main poppet. The symmetrical structure of the main poppet can ensure that the static pressure acting on the poppet is of balance.

The structure of the main poppet is shown in Fig. 5. Due to the good machinability, the non-circular opening structures

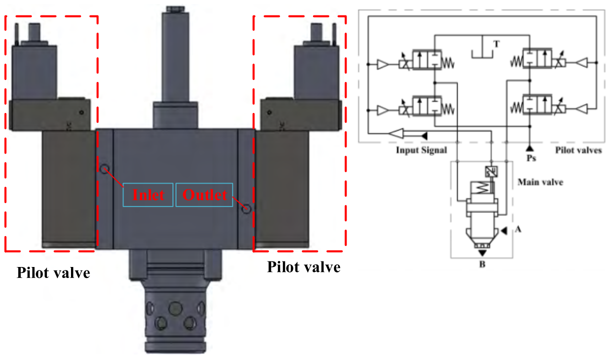

FIGURE 4. Principle of water hydraulic proportional cartridge valve.

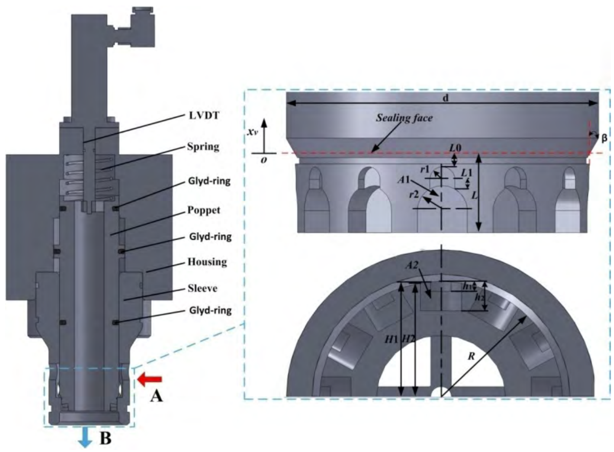

FIGURE 5. Main structure parameters of poppet.

with U-grooves are widely applied in the directional and proportional valves [27], [30]. And in order to make the die casting machine switch from slow-shot to fast-shot quickly, the non-circular opening structures with double-U-grooves are proposed. There are 12 double-U-grooves distributed uniformly on the poppet. The application of the double-U-grooves can help mitigate cavitation in the valve [14]. What's more, there will have a great change for the flow area gradient between the small U-grooves and the big U-grooves. And it is useful for the injection system to quickly switch from the slow shot phase to the fast shot phase.

The paper focuses on the flow field analysis and the optimization of major parameters presented in Fig. 5 to restrain influence of the nonlinear disturbance forces. These parameters have important effect on the nonlinear disturbance forces acting on the valve poppet. According to achieve the valve functionality, some of the parameters have a fixed value, such as $d = \Phi 50$mm, $R = 23.5$mm, $r_2 = 4$mm, $h_2 = 6$mm, $L = 12$mm, $L_0 = 2$mm. The allowable values of the parameters also are limited by requirements of the injection system (shown in Table 1). The decision parameters need to be optimized are: cone angle of the poppet β with the range from 20° to 60°, radius of the small U-grooves r_1 with the range from 1mm to 3mm, depth of the small U-grooves h_1 with the range from 1mm to 3mm, distance L_1 between the small U-grooves and the big U-grooves with the range from 1mm to 3mm. The initial values of the decision geometry parameters of the valve are: $\beta = 30°$, $r_1 = 2$mm, $h_1 = 2$mm, $L_1 = 1$mm. The throttling areas A_1 and A_2 of the double-U-grooves are shown in Fig. 5. A_1 is the flow area in radial and A_2 is the flow area in axial. Both of them are the function of the poppet opening x_v:

1.) When $L_0 \le x_v \le r_1 + L_0$

$$\begin{cases} A_{11} = 24 \displaystyle\int_{L_0}^{x_v} R \arcsin \frac{\sqrt{r_1^2 - (r_1 - x_v)^2}}{R} dx \\ A_{21} = 12(R^2 \arcsin \dfrac{\sqrt{r_1^2 - (r_1 - x_v)^2}}{R} \\ \quad + \sqrt{R^2 - (r_1^2 - (r_1 - x_v)^2}\sqrt{r_1^2 - (r_1 - x_v)^2} \\ \quad - 2\sqrt{r_1^2 - (r_1 - x_v)^2}(R - h_1)) \end{cases} \tag{1}$$

2.) When $L_0 + r_1 \le x_v \le L_0 + r_1 + L_1 + \sqrt{r_2^2 - r_1^2} - r_2$

$$\begin{cases} A_{12} = \max(A_{11}) + 24(x_V - (L_0 + r_1))R \arcsin \dfrac{r_1}{R} \\ A_{22} = \max(A_{21}) \end{cases} \tag{2}$$

3.) When $L_0 + r_1 + L_1 + \sqrt{r_2^2 - r_1^2} - r_2 \le x_v \le L_0 + r_1 + L_1$

$$\begin{cases} A_{13} = \max(A_{12}) \\ \quad + 24(x_V - (L_0 + r_1 + L_1 + \sqrt{r_2^2 - r_1^2} - r_2))R \arcsin \dfrac{r_1}{R} \\ A_{22} = \max(A_{22}) \\ \quad + 24(h_2 - h_1)\sqrt{r_2^2 - (L_0 + r_1 + L_1 + \sqrt{r_2^2 - r_1^2} - x_V)^2} \end{cases} \tag{3}$$

4.) When $L_0 + r_1 + L_1 \le x_v \le L_0 + r_1 + L_1 + \sqrt{r_2^2 - r_1^2}$

$$\begin{cases} A_{14} = \max(A_{13}) + 24 \int_{L_0 + r_1 + L_1}^{x_v} \\ \quad \cdot R \arcsin \dfrac{\sqrt{r_2^2 - (L_0 + r_1 + L_1 + \sqrt{r_2^2 - r_1^2} - x_v)^2}}{R} \\ A_{24} = 12(R^2 \arcsin \dfrac{\sqrt{r_2^2 - (L_0 + r_1 + L_1 + \sqrt{r_2^2 - r_1^2} - x_v)^2}}{R} \\ + (H_2 - 2(R - h_2))\sqrt{r_2^2 - (L_0 + r_1 + L_1 + \sqrt{r_2^2 - r_1^2} - x_v)^2} \end{cases} \tag{4}$$

5.) When $L_0 + r_1 + L_1 + \sqrt{r_2^2 - r_1^2} \le x_v \le L$

$$\begin{cases} A_{15} = \max(A_{14}) \\ \quad + 24R(x_v - (L_0 + r_1 + L_1 + \sqrt{r_2^2 - r_1^2})) \arcsin \dfrac{r_2}{R} \\ A_{25} = \max(A_{24}) \end{cases} \tag{5}$$

Equations (1)∼(5) are general formulae used for calculating the throttling areas of double-U-grooves. Based on the

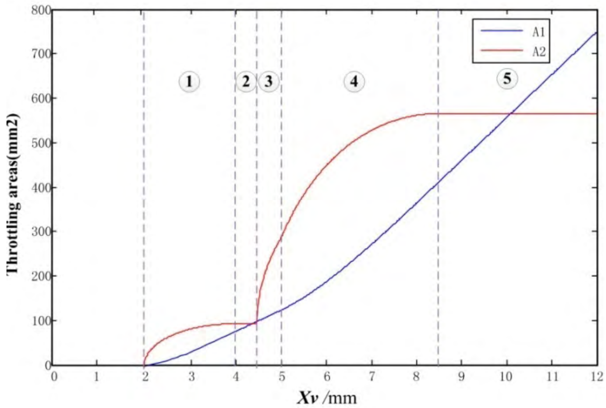

FIGURE 6. Throttling areas of double-U-grooves.

equations (1)~(5), the throttling areas A_1 and A_2 can be given as follows:

$$\begin{cases} A_1(x_v) = \sum_{i=1}^{5} A_{1i} \\ A_2(x_v) = \sum_{i=1}^{5} A_{2i} \end{cases} \tag{6}$$

Fig. 6 shows the relation between the flow areas (A_1 and A_2) and x_v. When the opening x_v is below L_0, the throttling areas, A_1 and A_2 is equal to zero. The water will effuse from the gap between the poppet and sleeve. Since the magnitude of the clearance is small, the flow is small. Therefore, the influence of the gap can be ignored. The throttling area A_2 increases monotonely with x_v through the full valve stroke. However, when $L_0 + r_1 \leq x_v \leq L_0 + r_1 + L_1 + \sqrt{r_2^2 - r_1^2} - r_2$ and $L_0 + r_1 + L_1 + \sqrt{r_2^2 - r_1^2} \leq x_v \leq L$, the throttling area A_2 will remain constant.

III. CFD COMPUTATIONAL MODEL

The first step for the analysis of CFD simulation is to build the 3D fluid models. The flow domain models with different valve openings would be designed by using Solidworks software. Then the model is imported to ANSYS for meshing generation using the FLUENT engine in a user friendly environment. The unstructured tetrahedral meshes are generated to overcome the complexity of the geometry.

In order to simulate the fluid dynamic behaviour in the entire range of the poppet stroke, the grid model is generated every 1mm of poppet displacement. Considering the limited space, only the maximal opening of the valve ($x_v = 12$mm) is shown in Fig 7. The mesh quality of the computational model is the key factor in obtaining the accurate result.

However, the higher accuracy usually requires more high quality grids, leading to more computing time. Considering the maximum velocity and pressure gradient occurring in the region of the valve opening, these refinements are mainly performed in the region of the valve opening. The good compromise between the need to reduce the computing time and maintaining high accuracy can be achieved by using local grid refinement. In the construction of the grid model there are approximately 1million elements and inflations 6 layers are used. The grid quality is rigorously checked, and the simulation results barely change as the amount of mesh increases.

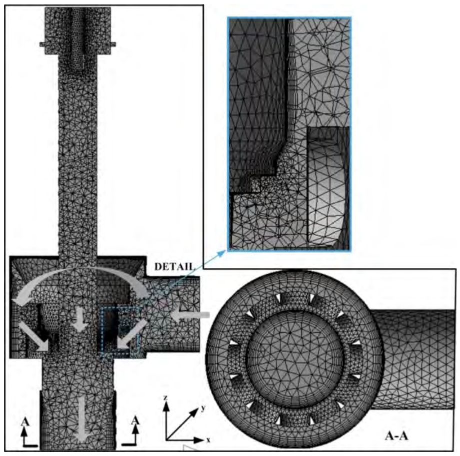

FIGURE 7. 3D grid model of flow domain.

IV. METHOD OF FLOW FORCE CALCULATION

Due to the large flow and high velocity in the metering edges, a turbulent flow pattern has been applied in the simulation calculation. In the ANSYS/FLUENT program [31] there are available turbulence model including: $k - \varepsilon$, $k - \Omega$ and Reynolds. Previous studies [32], [33] have proved that the $k - \varepsilon$ model can fit well in case of flow through the orifice of the control valve. There is little difference among these turbulence models (standard $k - \varepsilon$, RNK $k - \varepsilon$ and Realizable $k - \varepsilon$) in the turbulent flows simulation. So the standard $k - \varepsilon$ turbulence model has been applied to carry out turbulent flow simulation. The SIMPLE method is chosen to deal with velocity-pressure coupling. The SIMPLE algorithm has been widely used in numerous CFD applications since its robustness, low calculation cost and reasonable accuracy.

It is assumed that water is incompressible and its properties are constant. The water-liquid density and dynamic viscosity are set to $\rho = 998.2\text{kg/m}^3$ and $\mu = 0.001003\text{kg/m.s}$, respectively. On all walls no-slip boundary condition also has been assumed. Leakages and roughness of channel walls will be ignored. In the simulation, the inlet and outlet boundary types need be defined. The outlet boundary type is defined as pressure-outlet, and the pressure is fixed at 0.5MPa. For pressure inlet, the maximum pressure is 31.5MPa. The inlet boundary conditions are diverse, and it will be explained in detail later.

This study aims to reduce the flow forces by optimizing the geometry of the valve. The purpose is to reduce flow forces and improve the dynamic characteristics of the valve. Due to the small magnitude, gravity is ignored in the analysis. In the ANSYS/Fluent simulation, the hydraulic force acting on the poppet is computed by summing the pressure forces

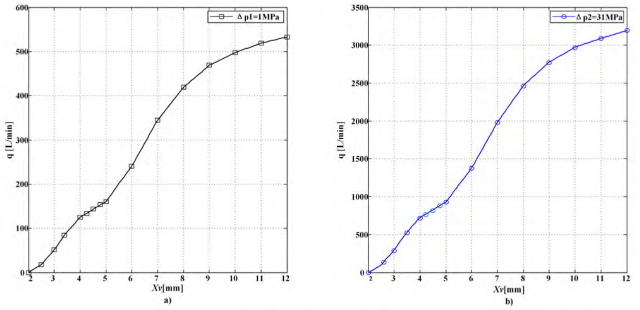

FIGURE 8. Flow rate results of the CFD simulation: a) $\Delta p_1 = 0.5$MPa b) $\Delta p_2 = 31$MPa.

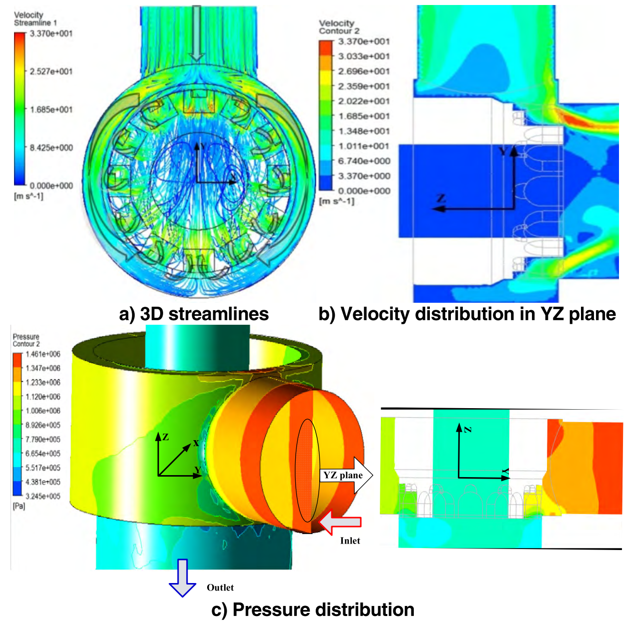

FIGURE 9. CFD simulation results of the initial model. a) 3D streamlines. b) Velocity distribution in YZ plane. c) Pressure distribution.

and viscous forces, as shown in the following equation

$$F_n = \vec{n}.\vec{F_p} + \vec{n}.\vec{F_v} \tag{7}$$

Where: F_n is the total hydraulic force along specified force vector, $\vec{n}$ is the specified force unit vector, $\vec{F_p}$ is the pressure force vector, $\vec{F_v}$ is the viscous force vector. Consequently, the hydraulic force includes two parts. One is the pressure force that acts on the surface of the poppet. The other is the viscous force generated as a result of the movement of the fluid that surrounds the poppet.

V. RESULTS AND DISCUSSIONS

The information about the values of flow forces can be obtained through CFD simulation, as well as the distribution of flow velocity and the pressure. In order to investigate the effects of geometry parameters on flow forces, the study gives some in-depth analysis on simulation results. For better understanding the simulation results, the initial fluid model with $r_2 = 4$mm, $h_2 = 6$mm, $L = 12$mm, $L_0 = 2$mm, $\beta = 30°$, $r_1 = 2$mm, $h_1 = 2$mm, $L_1 = 1$mm outlet pressure $p_{out} = 0.5$MPa, pressure difference $\Delta p_1 = 1$Mpa and $\Delta p_2 = 31$MPa is analyzed in detail. The numerical flow rate values of the initial model are shown in Fig. 8. It can be found that the flow rate increases with the increasing of the poppet stroke x_v. When the maximum pressure difference is equal to 31MPa, the maximum flow rate is 3200L/min. Regarding the dependence with the valve opening, it can be founded that the growth of flow rate is relatively flat between 4 and 5mm, 8 and 12mm, respectively. This is due to the fact that the throttling area A_2 remains constant in these two ranges (as shown in Fig. 6). Therefore, in these domains the throttling area A_2 restricts the growth of the flow rate. The discharge characteristic shown in Fig. 6 can satisfy the requirements of injection system, which control the speed of slow-shot and fast-shot in die casting machine. The flow forces acting on the poppet are the result of the pressure distribution and the flow velocity.

The streamlines and pressure distribution have been analyzed in the CFD simulations, shown as Fig. 9a-c.In the Fig. 9a, it can be found that the poppet acts as a barrier for the fluid flow. After entering from the inlet, the fluid flows in two directions: flow perpendicular to the poppet surface and flow going around the poppet and down towards the double-U grooves. Fig. 9b shows the velocity distribution in Y-Z plane. Fig. 9a and 9b indicate that the streamlines perpendicular to the poppet surface cause the separated flow going around the poppet and down towards the metering edge. The flow going round the poppet results in a low velocity profile, and the flow going down towards the grooves results in local velocity raise in the metering edge. As can be seen from the map (Fig. 9c) shown the pressure distribution, the pressure is distributed non-uniformly along the flow path. The large pressure difference occurs in the metering edge, while the velocity reaches a significant value about up to 33.7 m/s.

A. FLOW FORCE REDUCTION BY MEANS OF PARAMETER OPTIMIZATION

In order to reduce the flow forces, it is necessary to optimize the parameters of the metering edge that has the significant influence on pressure distribution. The simulation results presented in Fig. 10 show how the small U-grooves radius r_1 affects the axial flow forces at different inlet flow rate when the poppet stroke is 12mm.The axial flow forces as the function of r_1 and inlet flow rate q are shown in Fig. 10a.

When the inlet flow rate is equal to the maximal value 3200L/min, the axial flow forces reach the maximal value. Fig. 10b shows the axial flow forces as the function of the small U-grooves radius r_1 for $q = 3200$L/min. The initial radius $r_1 = 1$mm results in the minimal axial flow forces 4533.3N. The axial flow forces increases with the increasing of r_1. When r_1 is equal to 2mm, the axial flow forces reached the maximum value about up to 4725.2N. When r_1 is varying from 2mm to 3mm, the axial flow

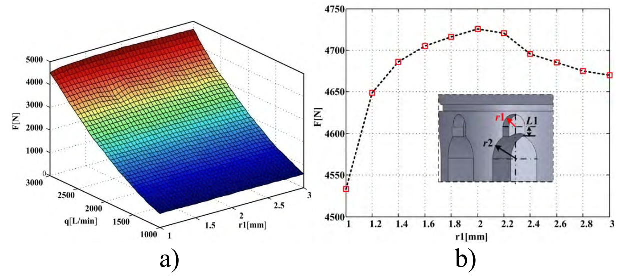

FIGURE 10. The simulation results of flow forces: a)flow forces against r_1 with different flow rate b)flow forces as a function of r_1 with $q = 3200$L/ min.

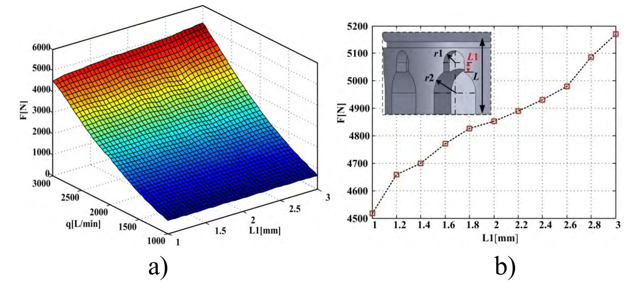

FIGURE 12. The simulation results of flow forces: a) flow forces against L_1 with different flow rate b) flow forces as a function of L_1 with $q = 3200$L/min.

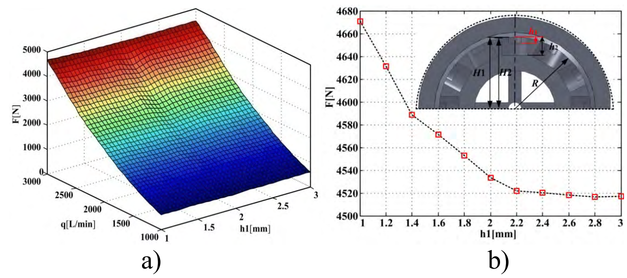

FIGURE 11. The simulation results of flow forces: a) flow forces against h_1 with different flow rate b) flow forces as a function of h_1 with $q = 3200$L/min.

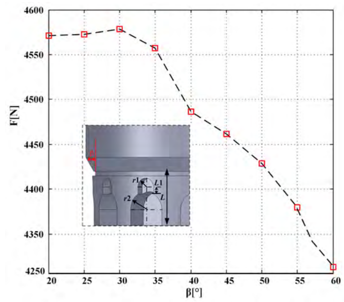

FIGURE 13. The Flow forces as the function of cone angle β of the poppet with $q = 3200$L/ min.

forces have fallen only marginally to 4670.2N. In this case, $r_1 = 1$mm represents the point effecting on major reduction of the axial flow forces from 4725.2 to 4533.3N (as shown in Fig. 10b). The axial flow forces have been reduced by 4.1%. Therefore, the simulation model with $r_1 = 1$mm is chosen for the further analyses.

Fig. 11 shows the influence of the small U-grooves depth h_1 on the axial flow forces when $x_v = 12$mm. The axial flow forces as a function of t h_1 and inlet flow rate q are shown in Fig. 11a. The maximal flow forces is achieved at maximal inlet flow rate, therefore, the simulated results of the axial flow forces can be described as a function of the depth h_1 at maximal inlet flow rate $q = 3000$L/min. The axial flow forces decreases with the increasing of the depth h_1 with the range from 1mm to 2.2mm, while varying the depth from 2.2mm to 3mm does not have a significant influence on axial flow forces (Fig. 11b). It can be found that the minimal flow forces can be achieved at $h_1 = 3$mm, where the axial flow forces have been reduced from 4671N to 4517.3N (reduced by 3.3%). So, $h_1 = 3$mm is chosen for the models involved in further analyses.

Fig.12a reports the distance L_1 between the small U-grooves and the big U-grooves and the inlet flow rate q as a function of the axial flow forces in the case of $x_v = 12$mm. Fig. 12b shows the influence of the distance L_1 on axial flow forces at maximal inlet flow rate. The axial flow forces increases with the increasing of the distance L_1. The initial distance of 1mm results in a minimal axial flow forces $F = 4517.3$N. The distance L_1 has a major influence on axial flow forces. The CFD simulation results shown in Fig. 12b indicate that the reduction of axial flow forces of about 12.6% for the maximum flow can be achieved at $L_1 = 1$mm which is chosen for the further optimization.

The last parameter optimized in this paper is the cone angle β of poppet (Fig. 13). The cone angle β of poppet with the range from 20° to 60° are analyzed. The analyses indicate that it has no obvious effect on axial flow forces when cone angle β of poppet is small (less than 30°). However, when the cone angle $\beta \geq 30°$, the axial flow forces decrease with the increasing of the cone angle β. The minimal axial flow forces $F = 4252$N at $\beta = 60°$.

Based on guaranteeing the performance of the injection speed control system of the die casting machine, the final geometry parameters of the metering edge can be obtained: the small U-grooves radius $r_1 = 1$mm; the small U-grooves depth $h_1 = 3$mm; The distance between the small U-grooves and the big U-grooves $L_1 = 1$mm; the cone angle of poppet $\beta = 60°$. The maximum axial flow forces (when $x_v = 12$mm, $q = 3300$L/min) acting on the poppet has been reduced from 4725.2N to 4252N, and decreased by 10%.

The distance L_1 between the small U-grooves and the big U-grooves have remained the initial value 1mm unchanged. The flow forces with the initial parameters and the optimum parameters are shown in Fig. 14a and Fig. 14b respectively. As shown in Fig. 14c, it can be found that the difference between (a) and (b) is less than 3% when the valve opening $x_v \leq 4$mm, and the small U-grooves plays a major role on throttling action. However, when the valve opening

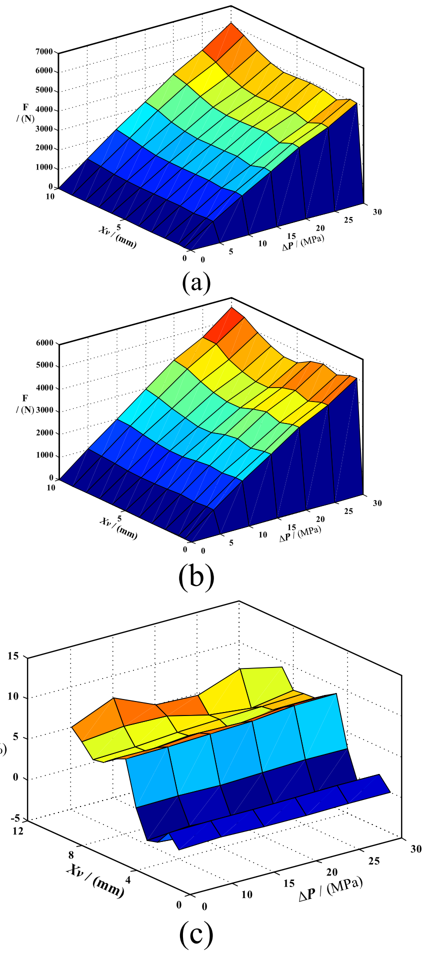

FIGURE 14. The flow forces under the whole stroke of the poppet; a) the flow forces with the initial parameters; b)the flow forces with the optimum parameters; c)the difference between a) and b).

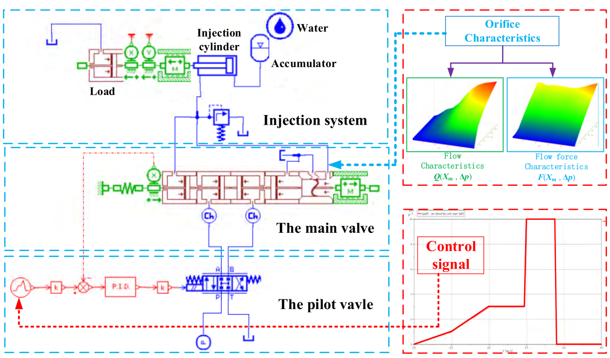

FIGURE 15. The simulation model of injection system.

$x_v \geq 4$mm, the small U-grooves and the big U-grooves work together as the two stage throttling orifice. The flow forces have been significantly reduced by optimizing the valve parameters.

B. SIMULATION OF THE INJECTION SYSTEM

Based on the principle of the injection system shown in Fig.3, the simulation model of injection system can be established

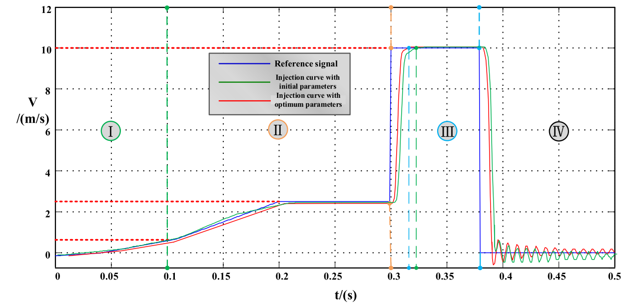

FIGURE 16. Injection process simulation.

by using AMESim R12.0 tool, as shown in Fig. 15. The response frequency and rated flow of the pilot valve are set as 100Hz and 40L/min respectively. The flow characteristic ($\boldsymbol{Q}(\boldsymbol{x}_{\mathbf{v}}, \Delta\boldsymbol{p})$) and the flow forces characteristic ($\boldsymbol{F}(\boldsymbol{x}_{\mathbf{v}}, \Delta\boldsymbol{p})$) can be obtain by CFD simulation. All that must be known is the table of the flow characteristic ($\boldsymbol{Q}(\boldsymbol{x}_{\mathbf{v}}, \Delta\boldsymbol{p})$) and the flow forces characteristic ($\boldsymbol{F}(\boldsymbol{x}_{\mathbf{v}}, \Delta\boldsymbol{p})$), and then the flow rate and flow forces can be obtained efficiently for a certain valve opening ($\boldsymbol{x}_{\mathbf{v}}$) and differential pressure ($\Delta\boldsymbol{p}$) condition. The injection process simulation results are shown in Fig. 16. The simulation results indicate that the optimum parameters of the poppet have little effect on injection control performance in slow shot phase I and II while the transition time from slow shot II to fast shot III has been almost reduced 6ms and accelerated stroke also has been shortened 16mm.

VI. CONCLUSION

In order to overcome the disadvantages of pollution, leakage, flammability and explosion, the die casting machine powered completely by water hydraulics is presented to replace the traditional one powered by oil hydraulics. The large flow and high response proportional valve as one of the most important hydraulic components in the die casting machine is introduced in section 2. In order to meet the flow rate requirements of slow-shot and fast-shot in the process of injection, a type of double-U-grooves structure is adopted. The precise mathematic model of flow area is established. And then the CFD simulation is conducted to obtain a better understanding on the pressure- flow characteristic of the non-circular opening valve with double-U-grooves. The CFD simulation results have confirmed that the pressure-flow characteristic of the double-U-grooves can satisfy the performance requirements of the injecting process.

The nonlinear factors such as fluid forces, friction forces and inertia forces have a significant influence on the dynamic characteristics and control precision of the large flow proportional valve. Moreover, these factors are typically associated with more energy consumption. Compared with other nonlinear disturbance forces, flow forces have more significant effect on the valve performance. Consequently, this study is focused on the reduction of the flow forces acting on the poppet, and proposed a numerical method for calculating the flow forces using CFD simulation on a three-dimensional model. The study demonstrated that the axial flow forces can be reduced by optimizing the geometry parameters of the grooves. By using the commercial software ANSYS/FLUENT, the optimal geometry of the double-U-grooves and the minimal axial flow forces are obtained. The axial flow forces increases with the increasing of the small U-grooves radius r_1 and the distance L_1 between the small U-grooves and the big U-grooves, while the increasing of cone angle β and depth h_1 can make the axial flow forces reduce. And the distance L_1 between the small U-grooves and the big U-grooves was found to have a major influence on the axial flow forces. With the help of the grooves geometry optimization, the maximum axial flow forces have been decreased by 10%.

At last, the simulation model of the simplified injection system has been established in AMESim. The simulation results proved that optimum parameters of the poppet can obviously improve the injection performance, and especially reduce the transition time form slow shot II to fast shot III. At the same time, accelerated stroke also has been shortened significantly.

REFERENCES

[1] Y. Liu, X. Zhao, D. Wu, D. Li, and X. Li, "Study on the control methods of a water hydraulic variable ballast system for submersible vehicles," *Ocean Eng.*, vol. 108, pp. 648–661, Nov. 2015.

[2] Y. Liu, X. Ren, D. Wu, D. Li, and X. Li, "Simulation and analysis of a seawater hydraulic relief valve in deep-sea environment," *Ocean Eng.*, vol. 125, pp. 182–190, Oct. 2015.

[3] W. Quan, Y. Liu, Z. Zhang, X. Li, and C. Liu, "Scale model test of a semi-active heave compensation system for deep-sea tethered ROVs," *Ocean Eng.*, vol. 126, pp. 353–363, Nov. 2016.

[4] W. Quan, Y. Liu, A. Zhang, X. Zhao, and X. Li, "The nonlinear finite element modeling and performance analysis of the passive heave compensation system for the deep-sea tethered ROVs," *Ocean Eng.*, vol. 127, pp. 246–257, Nov. 2016.

[5] D. Wu, Y. Liu, D. Li, X. Zhao, and X. Li, "Effect of materials on the noise of a water hydraulic pump used in submersible," *Ocean Eng.*, vol. 131, pp. 107–113, Feb. 2017.

[6] F. Johannaber, *Injection Molding Machines: A User's Guide*. New York, NY, USA: Hanser, 1994.

[7] C.-C. Tai, "The optimization accuracy control of a die-casting product part," *J. Mater. Process. Technol.*, vol. 103, no. 2, pp. 173–188, 2000.

[8] K. S. Lee and C. Luo, "Application of case-based reasoning in die-casting die design," *Int. J. Adv. Manuf. Technol.*, vol. 20, no. 4, pp. 284–295, 2002.

[9] J. C. Choi, T. H. Kwon, J. H. Park, and C. H. Kim, "A study on development of a die design system for diecasting," *Int. J. Adv. Manuf. Technol.*, vol. 20, no. 1, pp. 1–8, 2002.

[10] J. Y. Kumar, K. S. Amirthagadeswaran, and S. Gowrishankar, "Casting process optimization for reducing the cold shut defect in castings using response surface methodology," *Indian J. Eng. Mater. Sci.*, vol. 22, no. 2, pp. 187–194, 2015.

[11] Y.-M. Deng, D. Zheng, and X.-J. Lu, "Injection moulding optimisation of multi-class design variables using a PSO algorithm," *Int. J. Adv. Manuf. Technol.*, vol. 39, pp. 690–698, Nov. 2008.

[12] D. Wu, Y. Liu, D. Li, X. Zhao, and X. Ren, "The applicability of WC-10Co-4Cr/Si_3N_4 tribopair to the different natural waters," *Int. J. Refractory Metals Hard Mater.*, vol. 54, pp. 19–26, Jan. 2016.

[13] D. Wu, Y. Liu, D. Li, X. Zhao, and Y. Liu, "Tribo-corrosion properties of WC-10Co-4Cr coating in natural silt-laden waters when sliding against Si_3N_4," *Int. J. Refractory Metals Hard Mater.*, vol. 58, pp. 143–151, Aug. 2016.

[14] M. Han, Y. Liu, D. Wu, X. Zhao, and H. Tan, "A numerical investigation in characteristics of flow force under cavitation state inside the water hydraulic poppet valves," *Int. J. Heat Mass Transf.*, vol. 111, pp. 1–16, Aug. 2017.

[15] N. Herakovič, J. Duhovnik, and M. Šimic, "CFD simulation of flow force reduction in hydraulic valves," *Tehn. Vjesnik*, vol. 22, no. 2, pp. 453–463, 2015.

[16] R. Amirante, P. G. Moscatelli, and L. A. Catalano, "Evaluation of the flow forces on a direct (single stage) proportional valve by means of a computational fluid dynamic analysis," *Energy Convers. Manage.*, vol. 48, no. 3, pp. 942–953, 2007.

[17] R. Amirante, L. A. Catalano, and P. Tamburrano, "The importance of a full 3D fluid dynamic analysis to evaluate the flow forces in a hydraulic directional proportional valve," *Eng. Comput.*, vol. 31, no. 5, pp. 898–922, 2014.

[18] G. Del Vesoco and A. Lippolis, "A review analysis of unsteady forces in hydraulic valves," *Int. J. Fluid Power*, vol. 7, no. 3, pp. 29–39, 2006.

[19] M. Simic and N. Herakovic, "Reduction of the flow forces in a small hydraulic seat valve as alternative approach to improve the valve characteristics," *Energy Convers. Manage.*, vol. 89, pp. 708–718, Jan. 2015.

[20] E. Lisokwi, W. Czyzycki, and J. Rajda, "Three dimensional CFD analysis and experimental test of flow force acting on the spool of solenoid operated directional control valve," *Energy Convers. Manage.*, vol. 70, pp. 220–229, Jun. 2013.

[21] A. Hassanzadeh, M. S. Bakhsh, and A. Dadvand, "Numerical study of the effect of wall injection on the cavitation phenomenon in diesel injector," *Eng. Appl. Comput. Fluid Mech.*, vol. 8, no. 4, pp. 562–573, 2014.

[22] N. Pourmahmoud, M. Rashidzadeh, and A. Hassanzadeh, "CFD investigation of inlet pressure effects on the energy separation in a vortex tube with convergent nozzles," *Eng. Comput.*, vol. 32, no. 5, pp. 1323–1342, 2015.

[23] C.-C. Tsai, S.-M. Hsieh, and H.-E. Kao, "Mechatronic design and injection speed control of an ultra high-speed plastic injection molding machine," *Mechatronics*, vol. 19, no. 2, pp. 147–155, 2009.

[24] Tymac Process Automation LLC. *Principals of 7-Phase Real-Time Velocity Control*. Accessed: 2016. [Online]. Available: http://www.tymac.com/TymacProducts.html

[25] J. C. Ferreira, "A study of advanced die-casting technology integrating CAD/RP/FEA for Zn castings," *Int. J. Adv. Manuf. Technol.*, vol. 31, pp. 235–243, Nov. 2006.

[26] B. Xu, R. Ding, J. Zhang, and S. Qi, "Modeling and dynamic characteristics analysis on a three-stage fast-response and large-flow directional valve," *Energy Convers. Manage.*, vol. 79, pp. 187–199, Mar. 2014.

[27] *DSHR 2/2-Way Servo cartridge valve NB40, 50, 63, 80, 100, 125, 160*, Moog, Elma, NY, USA, 2016.

[28] *Proportional Throttle Valve-Series TDP, Catalogue HY11-3500/UK*, Parker, Cleveland, OH, USA, 2015.

[29] S.-H. Park, "Development of a proportional poppet-type water hydraulic valve," *Proc. Inst. Mech. Eng., C, J. Mech. Eng. Sci.*, vol. 223, no. 9, pp. 2099–2107, 2009.

[30] J. Zou *et al.*, "Cavitation in a non-circular opening spool valve with U-grooves," *Proc. Inst. Mech. Eng., A, J. Power Energy*, vol. 222, no. 4, pp. 413–420, 2008.

[31] *ANSYS FLUENT User's Guide Release 14.0*, ANSYS, Inc., Pittsburgh, PA, USA, 2011.

[32] B. E. Launder and D. B. Spalding, "The numerical computation of turbulent flows," *Comput. Methods Appl. Mech. Eng.*, vol. 3, no. 2, pp. 269–289, 1974.

[33] E. Lisokwi, G. Filo, and J. Rajda, "Pressure compensation using flow forces in a multi-section proportional directional control valve," *Energy Convers. Manage*, vol. 103, pp. 1052–1064, Oct. 2015.

MINGXING HAN received the B.S. and M.S. degrees in mechanical engineering from the Wuhan University of Technology, Wuhan, China, in 2009 and 2012, respectively. He is currently pursuing the Ph.D. degree with the School of the Mechanical Science and Engineering, Huazhong University of Science and Technology. His current research interests include water hydraulic components and systems and electro-hydraulic proportional control.

YINSHUI LIU received the B.S. and M.S degrees in mechanical engineering from the Lanzhou University of Technology, Lanzhou, China, in 1995 and 1998, respectively, and the Ph.D. degree in mechanical engineering from the Huazhong University of Science and Technology, Wuhan, China, in 2002. From 2002 to 2004, he was a Post-Doctoral Researcher with the College of Materials Science and Engineering, Huazhong University of Science and Technology. In 2004, he joined the School of the Mechanical Science and Engineering, Huazhong University of Science and Technology, where he has been a Professor, since 2009. He is currently the Director of the Department of Fluid Power Control Engineering, Huazhong University of Science and Technology. His current research interests include water hydraulics components and system, water mist technology, marine mechatronic systems, and hydraulic systems.

DEFA WU received the Ph.D. degree in mechatronic engineering from the Huazhong University of Science and Technology, Wuhan, China, in 2014. He was a Post-Doctoral Researcher with the College of Materials Science and Engineering, Huazhong University of Science and Technology. He is currently a Lecturer with the Huazhong University of Science and Technology. His current research is in dynamic control, underwater work tools, special hydraulic system, and industrial automation. His research in these areas builds on a large body of studies he pursued over the past 10 years and published in over 20 contributions.

HUAIJIANG TAN is currently pursuing the Ph.D. degree with the School of the Mechanical Science and Engineering, Huazhong University of Science and Technology. His main research interests include fluid power transmission and control.

CHAO LI received the B.S. degree in mechanical engineering from the Wuhan University of Technology, Wuhan, China. He is currently pursuing the master's degree with the School of the Mechanical Science and Engineering, Huazhong University of Science and Technology. His main research interests include fluid power transmission and control.